ELSEVIER

Thermochimica Acta 285 (1996) 231–241

thermochimica acta

The study of the glass transition in novolac resin by partial thermally stimulated depolarization current

M. Topić

Laboratory for Solid State Chemistry, Ruđer Bošković Institute, POB 1016, 10001 Zagreb, Croatia

Received 16 November 1995; accepted 13 February 1996

Abstract

The glass transition region of novolac phenol-formaldehyde (NPF) resin was investigated by integral and partial thermally stimulated depolarization current (TSDC). The experiments were performed on samples with admixtures which might influence the behaviour of the resin. The analysis of the activation energy vs. temperature showed three relaxation stages. Each stage was characterized by the relaxation map and the compensation temperature (T_c). The T_{c2} related to the middle stage coincided with the glass transition temperature (T_g), while the T_{c1} and T_{c3} were shifted. A model was proposed for unification of T_{c1} and T_g by including necessary changes in the relaxation parameters. For this purpose, an additional activation energy had to be introduced which was considered as the measure for the rigidity of the investigated system in certain temperature regions.

Keywords: Compensation phenomenon; Glass transition; Novolac phenol-formaldehyde; α-Relaxation; Thermally stimulated current

1. Introduction

The use of partitioning in the measurements of thermally stimulated depolarization current (TSDC) has become very popular as it enables one to divide a relaxation process into a series of elementary processes [1] and to obtain a real distribution of the relaxation parameters. The partitioning is based on the so-called "thermal windowing" experiments. An elementary depolarization process is produced by partial polarization within a narrow temperature window to isolate a narrow relaxation component [2]. The obtained data for relaxation time and temperature for each of the elementary processes are usually collected in the so-called relaxation map (RM) [3]. The RM is

PII: S0040-6031(96)02909-7

a set of Arrhenius lines

$$\ln \tau = \frac{E}{0.0862} \times \frac{10^3}{T} + \ln \tau_o \tag{1}$$

where τ is the relaxation time of an elementary peak, τ_o is the pre-exponential factor and E is the activation energy expressed in eV. If the Arrhenius lines converge to a single point, it is considered as the point of compensation with the coordinates: compensation temperature (T_c) and compensation relaxation time (τ_c). Usually, the polymer system has more than one T_c. Each T_c indicates a separate ordering in motion. The more distant the T_c's are, the greater the ordering segregation [4]. Generally, relaxation map analysis and the compensation phenomena can be used to characterize the polymers in quite a different way from other thermal analysis methods [5].

The integral TSDC investigation of pure novolac phenol-formaldehyde (NPF) resin was performed in 1978 [6]. The origin of peaks which appeared in the vicinity of T_g was explained and the distinction between the dipolar α-peak and the space charge ρ-peak was discussed [7,8]. The first TSDC study of NPF by use of the partial technique was performed in the β-temperature range from 137 to 270 K [9]. Analysis of the Arrhenius lines showed three different T_c's. One of them was very close to the glass transition temperature (T_g), while the other two were far away and were even irrational ($10^3/T_c < 0$). The T_c almost coinciding with T_g was explained as the consequence of the free motions not being inhibited by the surrounding structure. The irrational T_c's were explained in terms of inhibited motions. The presence of water in NPF significantly influenced the position of the T_c's [10]. All the motions were attributed to the rotation of the phenyl rings.

The aim of this paper was a more thorough study of the glass transition in NPF by use of partial measurements and the search for compensation phenomena. Another reason was to consider the physical meaning of the T_c's and the relation between T_c and T_g. Experiments were carried out with pure resin and the resin with additions. The samples were designed as follows: 1, pure resin; 2, resin with 10 wt% of $CaCO_3$, calcite; the crystal structure of $CaCO_3$ is centrosymmetric and, therefore, dipole–dipole interaction between the resin and the filler is excluded; 3, resin with 10 wt% tartaric acid anhydride (TAA); the crystal grains of TAA possess a permanent dipole [11].

2. Experimental

The preparation of NPF resin was described in a recent paper [9]. The $\bar{M}_n$ was 603. The T_g determined by DSC was 334 K. The fillers were analytical grade crystalline powders with non-defined particle sizes. The resin and filler were mixed and ground in a mortar. The mixtures were melted at 373–383 K for 15 min. The samples were 13.6 mm in diameter and 1 mm thick with silver-coated brass electrodes. Other details are given elsewhere [6,12]. The integral TSDC measurements were performed in the following way: preheating up to 373 K in the short-circuited state (s.c.s.), polarization by an electric field $E_p = 4\ \text{kV cm}^{-1}$ at $T_p = 333$ K for 20 min, cooling to the temperature $T_0 = 298$ K under E_p, storage relaxation at T_0 in the s.c.s. for 30 min, and depolariz-

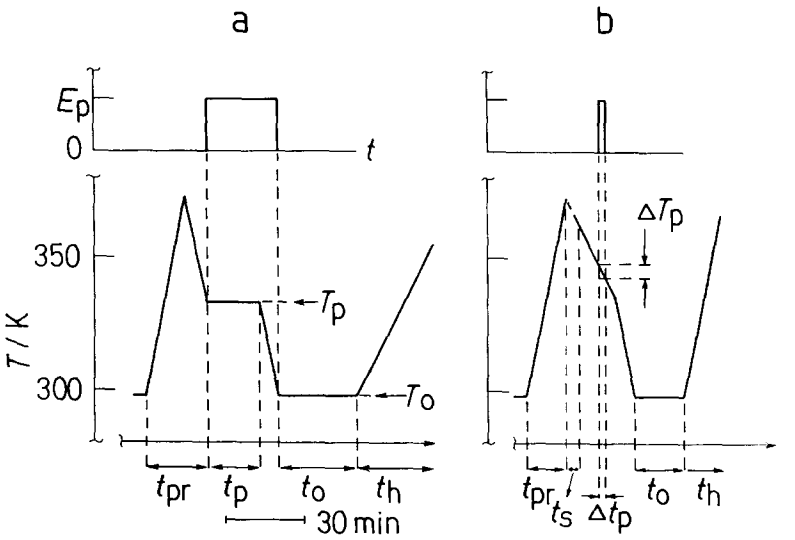

Fig. 1. (a) Procedure for integral TSDC measurements: E_p, polarization field; T_p, polarization temperature; T_0, storage temperature; t_{pr}, time of preheating; t_p, polarization time; t_0, storage time; t_h, heating time for current stimulation. (b) Procedure with the partial polarization: ΔT_p, partial polarization temperature; t_s, time for stabilization of cooling rate; Δt_p, partial polarization time.

ation by heating. The cooling rate was 5 K min^{-1} and heating rate 2 K min^{-1}. The runs with the partial polarization were performed differently: preheating up to 373 K, cooling to various T_p in the s.c.s. (2 K min^{-1}), cooling under $E_p = 4$ kV cm^{-1} from T_p to $T_p - 5$ K (2 K min^{-1}), cooling to T_0 in the s.c.s. (5 K min^{-1}) and storage at T_0 in the s.c.s. The time of cooling and storage together was 30 min. Depolarization was performed by heating at 5 K min^{-1}. In comparison with the recent paper [9], the partial polarization was simplified so that the E_p was applied just during continuous cooling in the $T_p - 5$ K $= \Delta T$ "window". The same approach was used successfully by other authors [13]. For a better understanding of the experimental procedure, the related E_p, $T(t)$ diagrams are drawn in Fig. 1. Diagram (a) is related to the integral runs while (b) is related to a typical run with the partial polarization performed at $\Delta T_p = 348$–343 K as an example. The current was measured by a Keithley 617 electrometer.

3. Results and discussion

3.1. Integral TSDC measurements

Depolarization curves of a freshly prepared batch of pure NPF and of NPF with fillers are shown in Fig. 2. The integral measurements in the α-range were performed in order to obtain a preliminary insight into the influence of the admixtures. The relatively low T_p of 333 K was chosen in order to avoid the occurrence of the Satellite ρ-peaks.

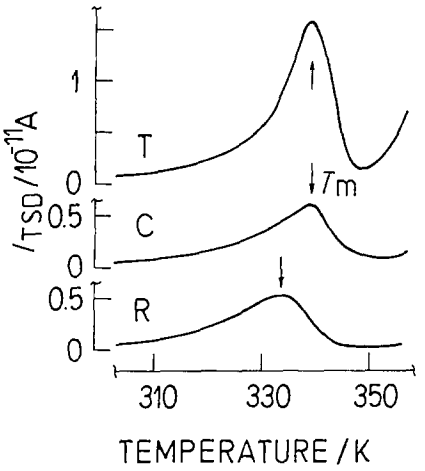

Fig. 2. Plot of TSDC versus temperature for different samples: R, NPF resin; C, resin with $CaCO_3$; T, resin with tartaric acid. $E_p = 4$ kV cm^{-1}, $T_p = 333$ K. T_m, temperature of the peak maximum.

The curve R with maximum at $T_m = 334$ K was obtained with pure resin. The curve C is for resin filled with calcium carbonate. The curve T is for resin filled with TAA. One can see that the addition of calcium carbonate has practically no influence on the depolarization process. Only T_m is slightly shifted to 339 K, probably due to the change of thermal conductivity in the sample. The addition of 10 wt% TAA increases the maximum current (I_m) three times. One can assume that hydrogen bonding between the components takes place which increases the dipole moments of the moving parts in the resin.

3.2. *Partial polarization*

Partial polarization was performed on samples R, C and T. The temperature range from 288 to 348 K was partitioned into a series of elementary peaks. The peaks were normalized by subtraction of the parasitic current [12] and the net values for I_m are shown in Fig. 3.

The activation energy E of the elementary peaks was determined by the Christodoulides method [9,14] using the equation.

$$E = \frac{T_1 T_m}{7940(T_m - T_1)} - \frac{T_1}{14866} \tag{2}$$

where T_1 is the temperature related to $I_m/2$ (low temperature side) and T_m is the temperature of the elementary peak maximum. As the peak is obtained in a relatively narrow temperature interval, the calculated E can be approximated as a unique value for the entire elementary peak. The values of E versus T_m are shown in Fig. 4. Despite some dispersion of the points, one may consider two distinctive groups of points and

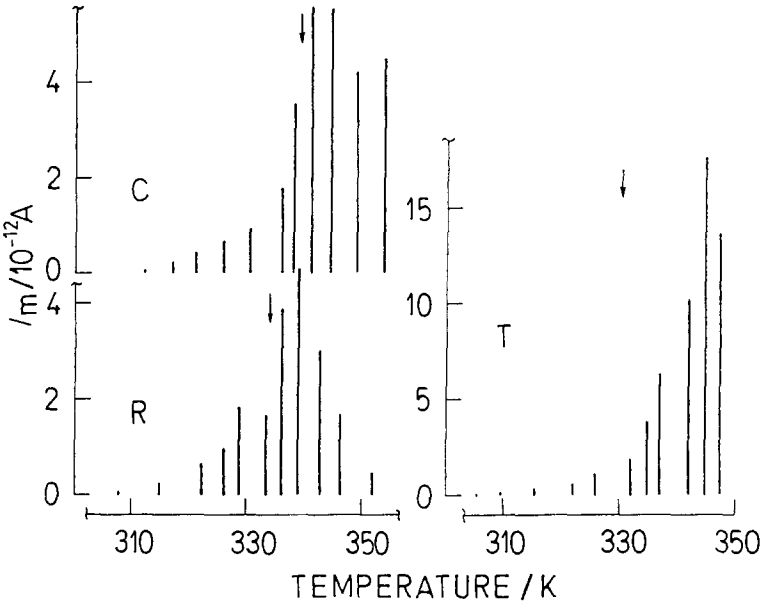

Fig. 3. Parameters of elementary peaks obtained by partial polarization. Symbols of samples as in Fig. 1. Arrows are related to T_m obtained in integral measurements.

draw the most probable lines l_1 and l_3 for all three samples. It was also possible to introduce an additional middle line l_2 between l_1 and l_3; l_2 is defined by points P and P′ in Fig. 4. In the determination of l_3 for sample R, the deviated point at $T_m = 343$ K was neglected. In further analysis, the elementary E values were replaced by E_l values which fit the drawn lines.

All the elementary peaks up to the maximum E are related to the α depolarization process while the last high temperature peaks are related to the satellite space charge ρ-process. In spite of the origin of the released charge, all the results in Fig. 4 represent the entire energy course of the glass transition. The changes in dielectric behaviour are a reflection of the changes in the order of the molecular motions.

3.3. *Relaxation map analysis*

Fig. 5 shows the RM for pure resin. In general, a relaxation line can be drawn on the basis of a few values for $\ln \tau(T)$ of an elementary peak and extrapolated to the compensation point [3]. We determined each of the relaxation lines by two independent values, a point and a slope, which can be obtained with the highest possible accuracy [9]. The upper points are related to the T_m of the elementary peaks. The related $\tau(T_m)$ values are obtained by the equation

$$\tau(T_m) = Q(T_m)/I_m \tag{3}$$

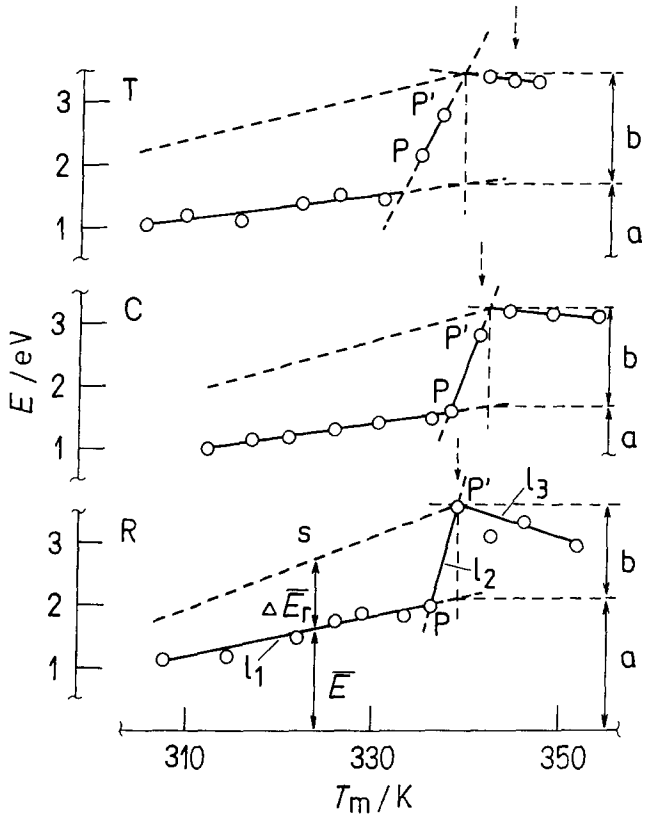

Fig. 4. E versus T_m for different samples, related to the elementary peaks in Fig. 2: l_1, l_2 and l_3 are fitting lines, s, simulated line; P and P', spanning points; a/b, ratio of the energy jump; $\bar{E}$, average activation energy for l_1 range; $\Delta\bar{E}_r$, additional average energy to achieve simulated function. Dashed arrows are related to the elementary peaks with maximum amplitude in Fig. 2.

where $\tau\,(T_m)$, $Q(T_m)$ and I_m are the relaxation time, residual charge and current at the peak maximum, respectively. The slopes are determined from E_1.

The RM can be drawn or approved mathematically by use of the so-called compensation line equation [15]

$$\ln \tau_o = -\frac{10^3}{T_c} \times \frac{E_1}{0.0862} + \ln \tau_c \tag{4}$$

This represents a linear function $\ln \tau_o(E_1)$ in which the negative slope is equal to $10^3/0.0862\ T_c$, while the intercept is equal to $\ln \tau_c$. The related $\ln \tau_o$ is determined by Eq. (1).

As regards the sample R, the initial stage of relaxation related to the line l_1 from Fig. 4 shows the compensation at $T_{c1} = 363$ K. For the final part of the relaxation related to l_3, the Arrhenius lines are divergent, showing the compensation at

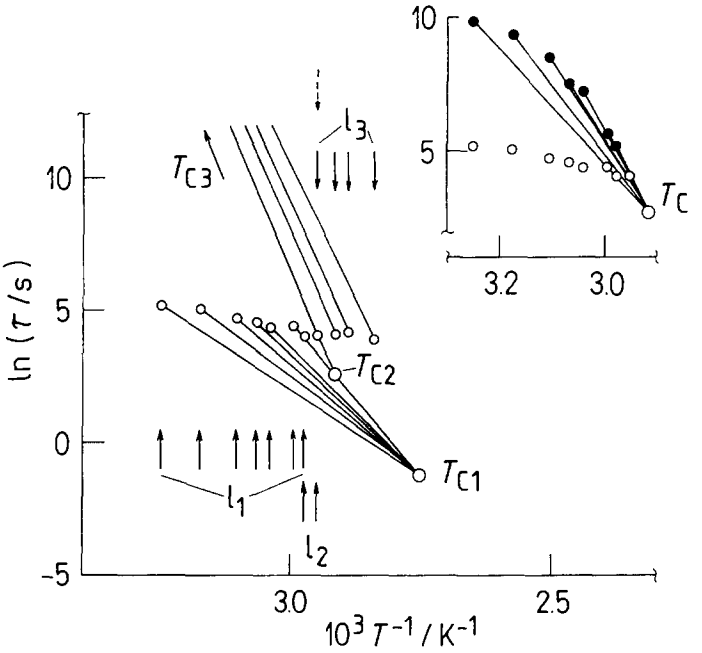

Fig. 5. Relaxation map (RM) ln τ versus $10^3/T$ for NPF resin: l's, temperature regions related to fitting lines in Fig. 3; T_c's, compensation points. Arrows show T_m of the elementary peaks. Dashed arrow is related to the maximum amplitude peak. Inset: simulated RM with the unique T_c for l_1 and l_2 regions: ○, experimentally obtained τ; ●, simulated τ.

$T_{c3} = 288$ K. It is interesting to examine the middle l_2 stage and to determine the related compensation point with only two Arrhenius lines. The compensation T_{c2} occurs at 343 K which is close to T_g. Taking into account the differences between the two techniques (TSDC and DSC), T_{c2} can be approximated to be equal to T_g. The highest slope of l_2 in the $E(T_m)$ function corresponds to the highest change in entropy of the entire relaxation process. This is in agreement with the standpoint that T_g occurs at the maximum of entropy and enthalpy [16]. Instead of the enthalpy of activation (ΔH), we write the energy of activation. If one takes

$$E = \Delta H + RT \tag{5}$$

and knowing that RT is equal to 0.026 eV at room temperature, the energy is practically equal to the enthalpy. In general, for a certain temperature rate in the TSDC runs, the position of T_g obtained in the described way is dependent on the accuracy of the parameters of the elementary peaks as well as on the width of the "temperature windows".

The RM for samples C and T is shown in Figs. 6 and 7, respectively. The compensation parameters T_c and τ_c are listed in Table 1. In the initial stage of relaxation for all the samples, the Arrhenius lines are convergent, giving T_{c1} higher than T_g. The difference $T_{c1} - T_g$ increases from sample R across C to sample T.

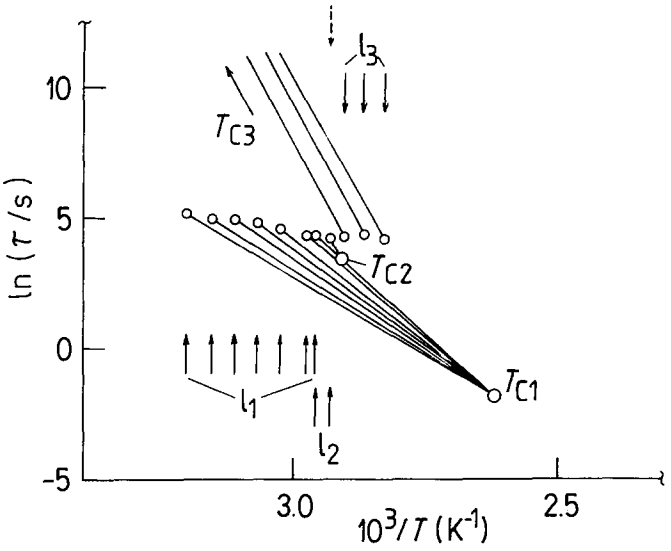

Fig. 6. RM for resin with $CaCO_3$.

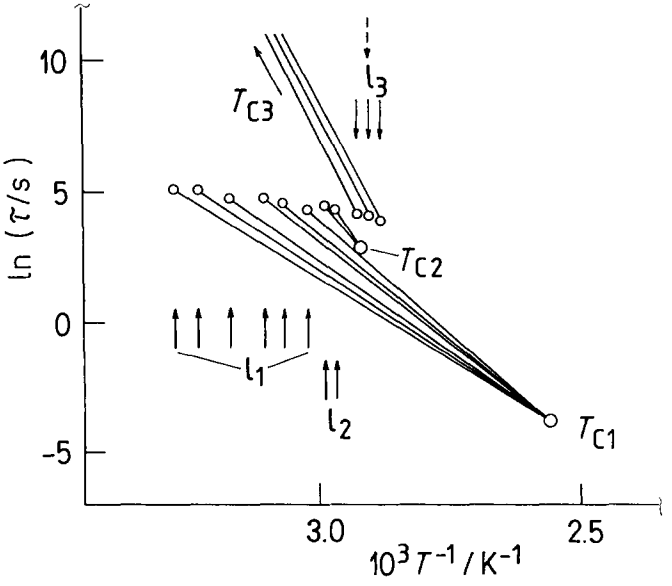

Fig. 7. RM for resin with tartaric acid.

According to the recent discussion [9], the position of T_c in general depends on the whole structure interference with molecular motion. Such a conclusion can be supported by the general discussion about the influence of the hindered molecular mobility on T_c [16]. The difference $T_{c1} - T_g$ is an indication of the width in the distribution of E,

Table 1
Comparison of results for compensation temperature (T_c), compensation relaxation time (τ_c), factor of energy jump (f), average activation energy in l_1 region ($\bar{E}$) and related average energy of internal interference ($\overline{\Delta E_r}$) for different sample

Samples	T_{c1}/K τ_{c1}/s	T_{c2}/K τ_{c2}/s	T_{c3}/K τ_{c3}/s	f	$\bar{E}$/eV	$\overline{\Delta E_r}$/eV
R	363 0.29	343 14.0	288 1.2×10^{11}	1.73	1.6	1.15
C	382 0.16	344 32.8	199 6.9×10^{35}	1.94	1.3	1.2
T	391 0.023	343 17	236 2.8×10^{24}	2.06	1.3	1.4

[a] Approximately coincides with T_g.

showing the variety in the molecular motions of the resin. At higher T_{c1}, a lower variety in the motions exists. The highest T_{c1} obtained for sample T can be explained as being caused by the hydrogen bonding between TAA and NPF. In contrast, the Arrhenius lines for the l_3 region are divergent (in relation to the increasing T), giving T_c's way below the T_g value. This is a consequence of the post-transition state in the polymer in which the change in E versus T_m is very small or even negative. Such a behaviour was also present in the β-relaxation of NPF at the end of the relaxation process [9].

3.4. *Unification of T_c and T_g*

Considering T_g as the temperature of the cooperative motion, the T_g itself is the compensation point at which the different tendencies of motion are unified. A question arises as to how to explain the occurrence of various T_c's and their shift in relation to T_g. This problem was discussed in the previous paragraphs. As a contribution to this discussion, let us analyse once again the initial stage of relaxation in sample R. The function $E(T_m)$ was one of the main factors for determination of the related RM. For the region l_1, the obtained T_{c1} occurred at a temperature higher than T_g, but for l_2 the value of T_{c2} was practically equal to T_g. The shift of T_{c1} towards higher temperatures was proposed to be caused by an internal structure interference. What should one change in the function $E(T_m)$ for l_1 in order to unify regions l_1 and l_2, and achieve $T_{c1} = T_{c2} = T_g$? The first step is the introduction of a new simulated energy (E_s) which could overcome the structure interference

$$E_s = E_1 + \Delta E_r \tag{6}$$

where ΔE_r is the additional energy required for compensation of the surrounding structure interference. To draw a new RM with the unified regions l_1 and l_2, a simulated equation is proposed

$$\ln \tau + \Delta \ln \tau = \frac{E_1 + \Delta E_r}{0.0862} \times \frac{10^3}{T} + \ln \tau_o + \Delta \ln \tau_o \tag{7}$$

or

$$\ln \tau_s = \frac{E_s}{0.0862} \times \frac{10^3}{T} + \ln \tau_{os} \tag{8}$$

The simulated parameters with the subscript s are determined as follows. E_s can be calculated from

$$E_s = E_1 \times f \tag{9}$$

and

$$f = \frac{a+b}{a} \tag{10}$$

where f is the factor of the energy jump in the l_2 region, while a and b are defined in Fig. 4. The simulated line $E_s(T_m)$ is drawn as line s in Fig. 4. The remained τ_s can be obtained by use of the compensation law [15]

$$\ln \tau = \frac{E}{0.0862}\left(\frac{10^3}{T} - \frac{10^3}{T_c}\right) + \ln \tau_c \tag{11}$$

with the simulated values for E, τ and the unique $T_c = T_g$

$$\ln \tau_s = \frac{E_s}{0.0862}\left(\frac{10^3}{T} - \frac{10^3}{T_g}\right) + \ln \tau_g \tag{12}$$

Now it is possible to draw the simulated RM for sample R which is shown in the inset of Fig. 5 in which all the Arrhenius lines of the l_1 and l_2 regions are gathered into a unique $T_c = T_g$. Such an analysis was performed for samples C and T as well. According to Eqs. (6) and (9), the proposed energy of internal interference ΔE_r is

$$\Delta E_r = E_1(f - 1) \tag{13}$$

For the comparison of different samples, the mean $\Delta \bar{E}_r$ for the l_1 region was calculated and is given in Table 1. Finally, one can conclude that the shift of T_{c1} in comparison to T_g occurred because the Brownian motion is not sufficient to overcome the resistance in the matrix during the initial stage of relaxation. This additional energy could be a measure of the rigidity in the investigated amorphous polymer systems. Therefore, the results of $\Delta \bar{E}_r$ show an increase from sample R across C to sample T. The last case is probably caused by the hydrogen bonding at the interfaces between the resin and TAA.

4. Conclusions

The integral TSDC measurements of NPF across the glass transition were performed on samples with different admixtures which might interfere with the behaviour of resin. The addition of 10 wt% of TAA caused a three-fold in I_m. This was explained in terms of the interaction of the polar TAA with the moving parts of NPF which increased the polarizability in the resin.

Other measurements were performed by partial polarization in which the glass transition range was covered by 11 separate runs. The elementary peaks obtained were defined by E and $\tau(T_m)$. The analysis of the $E(T_m)$ function shows three different linear stages l_1, l_2 and l_3. This enables one to draw the related RM's and to determine the related T_c's. The initial stage l_1 shows the T_c's at higher temperatures than T_g, while the final regions, l_3, show T_c's at lower temperatures than T_g. The T_{c2}, which is related to the span between the stages l_1 and l_3, was practically equal to the T_g. It is proposed that the shift in T_c's in relation to T_g is a consequence of the hindered molecular motions caused by the interference with the surrounding resin structure. An attempt was made to model a simulated RM for stage l_1 in which T_{c1} would be equalized to T_{c2}, e.g. T_g. For that purpose the relaxation parameters were modified and an additional energy ΔE_r had to be taken into account. ΔE_r might be understood as being equal to the energy of the internal interference and a measure for the rigidity of the investigated systems. The calculated ΔE_r for different samples showed a variation dependent upon the admixtures. The highest ΔE_r was found in resin mixed with TAA, possibly due to the hydrogen bonding.

Acknowledgements

The author would like to express his gratitude to Dr. Z. Katović for supplying the resin and to Professor S. Popović for simulating discussions and critical reading of the manuscript.

References

[1] K. Nishinari, D. Chatain and C. Lacabanne, J. Macromol. Sci. Phys., (B) 22 (1983) 529.
[2] C. Lacabanne, D. Chatain, J. Guillet, G. Seytre and J.F. May, J. Polym. Sci., Polym. Phys. Edn., 13 (1975) 445.
[3] A. Bernes, R.F. Boyer, D. Chatain, C. Lacabanne and J.P. Ibar, in S.E. Keinath, R.L. Miller and J.K. Rieke (Eds.), Order in the Amorphous State of Polymers, Plenum Press, New York, 1987, pp. 305–26.
[4] A. Saadat, A. Bernes, P. Cebeillac, A. Lamure, D. Chatain and C. Lacabanne, IEEE Trans. Electr. Insul., 25 (1990) 630.
[5] J.P. Ibar, Polym. Eng. Sci., 31 (1991) 1467.
[6] M. Topić, A. Moguš-Milanković and Z. Katović, Phys. Status Solidi (A), 86 (1984) 413.
[7] M. Topić, A. Moguš-Milanković and Z. Katović, Polymer, 28 (1987) 33.
[8] M. Topić, J. Polym. Sci., Polym. Phys. Edn., 24 (1986) 2209.
[9] M. Topić and Z. Katović, Polymer, 35 (1994) 5536.
[10] M. Topić and Z. Katović, Croat. Chem. Acta, 69 (1996), in press.
[11] S.B. Lang, in I. Lefkowitz and G.W. Taylor (Eds.), Ferroelectrics and Related Phenomena, Vol. 2, Gordon and Breach Sci. Publishers, New York, 1974, p. 76.
[12] M. Topić A. Moguš-Milanković and Z. Katović, Polymer, 32 (1991) 2892.
[13] C. Christodoulides, P. Pissis, L. Apekis and D. Daoukaki-Diamanti. J. Phys. (D) Appl. Phys., 24 (1991) 2050.
[14] C. Christodoulides, J. Phys. (D) Appl. Phys., 18 (1985) 1501.
[15] C. Lacabanne and D. Chatain, in Y. Wada, M.M. Perlman and H. Kokado (Eds.), Charge Storage, Charge Transport and Electrostatics with Their Applications, Elsevier, Amsterdam, 1979, pp. 312–16.
[16] J.P. Ibar and R.L. Gray, Proc. Am. Chem. Soc., Div. Polym. Mater: Sci. Engin., Fall Meeting 1993, Chicago, IL, USA, Vol. 69, pp. 76–7.